THE ASTROPHYSICAL JOURNAL, 345: L55–L58, 1989 October 1

EXPANDING MOLECULAR TORUS AROUND THE PLANETARY NEBULA IRAS 21282+5050

K. M. SHIBATA AND S. TAMURA
Astronomical Institute, Tohoku University

AND

S. DEGUCHI, N. HIRANO, O. KAMEYA, AND T. KASUGA
Nobeyama Radio Observatory, National Astronomical Observatory
Received 1989 May 24; accepted 1989 July 17

ABSTRACT

CO $J = 1$–0 emission at 115.271 GHz from the compact planetary nebula IRAS 21282+5050 has been mapped with the Nobeyama Millimeter Array with an angular resolution of about 4″. CO emission is elongated to the north and south, and peaks are seen at the north and south sides of the field center. The extent of CO emission in channel-velocity maps decreases with velocities away from the central velocity, and the position-velocity map along declination shows an asymmetric round structure surrounding the star position. These results indicate that CO gas in IRAS 21282+5050 forms an expanding torus whose axis lies along the east-west direction and is normal to the line of sight. The kinematical age of the torus is estimated to be about $2.1 \times 10^3 D$ yr, where D is the distance to IRAS 21282+5050 in kpc. Both from the ratio of the size of CO gas to that of ionized gas and from the intensity ratio of [O III] λ5007 to Hβ, we conclude that IRAS 21282+5050 is in earlier evolutionary stage of planetary nebula than NGC 7027 and NGC 2346.
Subject headings: interstellar: molecules — nebulae: individual (IRAS 21282+5050) — nebulae: planetary

I. INTRODUCTION

On the evolution of red giant stars into planetary nebulae, asymptotic giant branch (AGB) stars disperse their envelopes in circumstellar space and proceed into the stage of central stars of planetary nebulae. The investigation of the distribution and the velocity structure of the molecular gas around planetary nebulae or around proto–planetary nebulae gives us clues in understanding mass-loss mechanisms in the evolved stars and the subsequent formation and evolution of planetary nebulae. The sample of planetary nebulae in which CO emission is detected is not so plentiful (Mufson, Lyon, and Marionni 1975; Thronson and Mozurkewich 1983; Knapp 1985; Huggins and Healy 1986). Among these planetary nebulae, only NGC 7027 and NGC 2346, the relatively strong CO emitters, were mapped and investigated on their structures of molecular gas (Masson *et al.* 1985; Healy and Huggins 1988; Bachiller *et al.* 1989). Of the proto–planetary nebulae, CRL 2688 was mapped by CO and HCN (Heiligman *et al.* 1986; Kawabe *et al.* 1987; Bieging and Nguyen-Q-Rieu 1988).

IRAS 21282+5050 (hereafter IRAS 21282) has attracted our attention, at first, due to its strong emission features at 3.3, 3.4, 7.7, 8.6, and 11.3 μm which are promising candidates for hydrocarbon emission (de Muizon *et al.* 1986; Nagata *et al.* 1988). Subsequently, Cohen and Jones (1987) made spectroscopic observations of the starlike optical counterpart of IRAS 21282 in the optical region. Based on its low- and high-resolution spectra, they concluded that IRAS 21282 is a compact and unresolved planetary nebula which is in a modest-excitation class and has an O7(f)-[WC 11]–type central star with an extinction of 5.7 mag. Likkel *et al.* (1988) searched for radio emission from molecules in IRAS 21282 with the IRAM 30 m radiotelescope and detected strong emission from CO ($J = 1$–0 and $J = 2$–1) and weak emission from ^{13}CO ($J = 1$–0) and HCO^+ ($J = 1$–0). They also derived the size of CO around IRAS 21282 as about 10″ in diameter from the CO ($J = 2$–1) map. As the instrumental resolution in CO ($J = 2$–1) was 12″, smaller structures were not resolved. If IRAS 21282 is a young planetary nebula as described by Cohen and Jones (1987), it is an excellent example for investigating the early stage of planetary nebula formation based upon both radio and optical data.

In order to analyze the structure of the ejected material around IRAS 21282, we have made a high-resolution interferometric map of CO $J = 1$–0 emission. We present the results on the structures of molecular gas and discuss the evolutionary stage of IRAS 21282.

II. OBSERVATIONS AND RESULTS

We have oserved CO $J = 1$–0 emission at 115.271 GHz from IRAS 21282 with the Nobeyama Millimeter Array (Ishiguro *et al.* 1984) on 1988 December 15 and 1989 January 28.[1] The observations were made with two configurations of five 10 m antennas giving a total of 20 independent baselines. The maximum and the minimum values of antenna separation were 129 m and 20 m, respectively. The total on-source integration time was 7.6 hr. The antennas were installed with SIS receivers, providing a system temperature (SSB) of about 600 K at 115 GHz. The backend was a 1024 channel digital FFT spectro-correlator, called FX (Chikada *et al.* 1987). We used an FX bandwidth of 320 MHz, which gave a total velocity coverage of 833 km s^{-1} and a velocity resolution of 0.81 km s^{-1}. The primary beam of the single antenna had a size of 1′ in diameter (HPBW) and was centered on the position of IRAS 21282, $\alpha = 21^h28^m15\overset{s}{.}1$, $\delta = +50°50'47''$ (1950.0, de Muizon *et al.* 1986).

[1] This work was carried out under the common use observation program at the Nobeyama Radio Observatory (NRO). NRO is a branch of the National Astronomical Observatory, an inter-university research institute operated by the Ministry of Education, Science, and Culture, Japan.

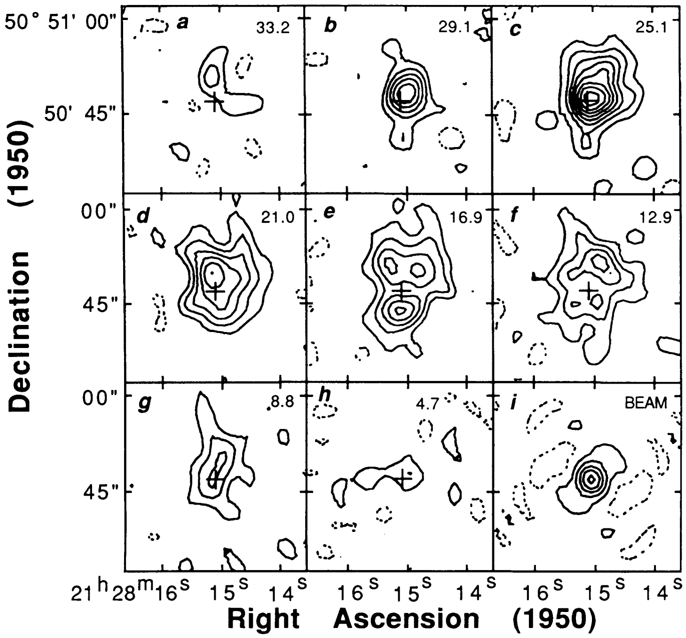

FIG. 1.—CLEANed maps of CO $J = 1–0$ emission in IRAS 21282+5050. Each map was averaged over five channels. The panels are labeled with the LSR velocities. The position of IRAS 21282+5050 (de Muizon *et al.* 1986) is marked with the cross. Contour levels are in linear steps of 0.6 Jy $beam^{-1}$ (2 σ level of the maps) and broken contours are for negative intensities. The synthesized beam is presented in panel (*i*), in which the contour levels are −10, 10, 30, 50, 70, and 90% of the peak intensity.

BL Lac was used as an amplitude and phase calibrator and 3C 84 as a bandpass calibrator. The observed visibility data were Fourier-transformed and CLEANed by using the Astronomical Image Processing System (AIPS), which is installed on computers of the Nobeyama Radio Observatory.

In Figure 1, we present eight maps of CO $J = 1–0$ emission which were obtained by five-channel averaging corresponding to a velocity resolution of 4 km s^{-1}. After applying a Gaussian taper of 60 kλ, the synthesized beam had a size of 4".1 × 3".6 (HPBW) with a position angle of 9°.6 and is shown in Figure 1*i*. The strongest emission is seen in Figure 1*c*, which has higher radial velocity than the central velocity of CO $J = 1–0$ emission around IRAS 21282 ($V_{LSR} = 18.0$ km s^{-1}; Likkel *et al.* 1988). Also, we can see that the integrated flux is stronger in the high-velocity part (with respect to the central velocity) than that in the low-velocity part. Probably this is due to a self-absorption of CO. The total flux of CO emission in our interferometric measurement is about 52% of the single-dish flux measured by Likkel *et al.* (1988). In each panel, except Figures 1*a* and 1*h*, overall elongation in the north-south direction is seen in the emission contours.

Three peaks are found in Figure 1*e*. One peak is situated at the south, and another two are at the north from IRAS 21282. The south peak and the two north peaks are about 7".5 apart in the north-south direction and the north peaks are 4".7 apart each other in the east-west direction. The northeast peak connects to a peak in Figure 1*d*, and the northwest peak connects to the stronger peak in Figure 1*f*.

We can see that the size of the emission region in each panel decreases with velocities away from the central value. Further, it should be noted that the positions of the center of emission in all panels of Figure 1 (the center of gravity of the contour at the level of 1.2 Jy $beam^{-1}$) coincide within 1" and the mean position of these centers is 0".3 west and 1".9 north from the field center. No systematic displacement of center positions is found.

In Figures 2*a* and 2*b*, we show position-velocity diagrams at position angles of 0° and 90° through the field center. We also present the position of the central star of IRAS 21282 in the diagrams. According to Cohen and Jones (1987), the radial velocity of ionized gas (Hα and [N II] lines) is $V_{LSR} = 17$ km s^{-1}. We suppose this velocity to be the velocity of the central star and the star position referred to de Muizon *et al.* (1986). In Figure 2*a*, a strong peak of emission is seen at the velocity of 26 km s^{-1}, and this peak corresponds to the emission peak seen in Figure 1*c*. Two ridges are seen from that strong peak; one extends to the bottom left and reaches a weaker peak, and the other extends to the top left. These peaks and ridges form the round shape which surrounds the star position with an asymmetric structure breaking off in the approaching side. In Figure 2*b*, we also find the strong peak and a weak peak corresponding to the strong peak and the top left ridge in Figure 2*a*, respectively.

In order to examine whether radio continuum emission is

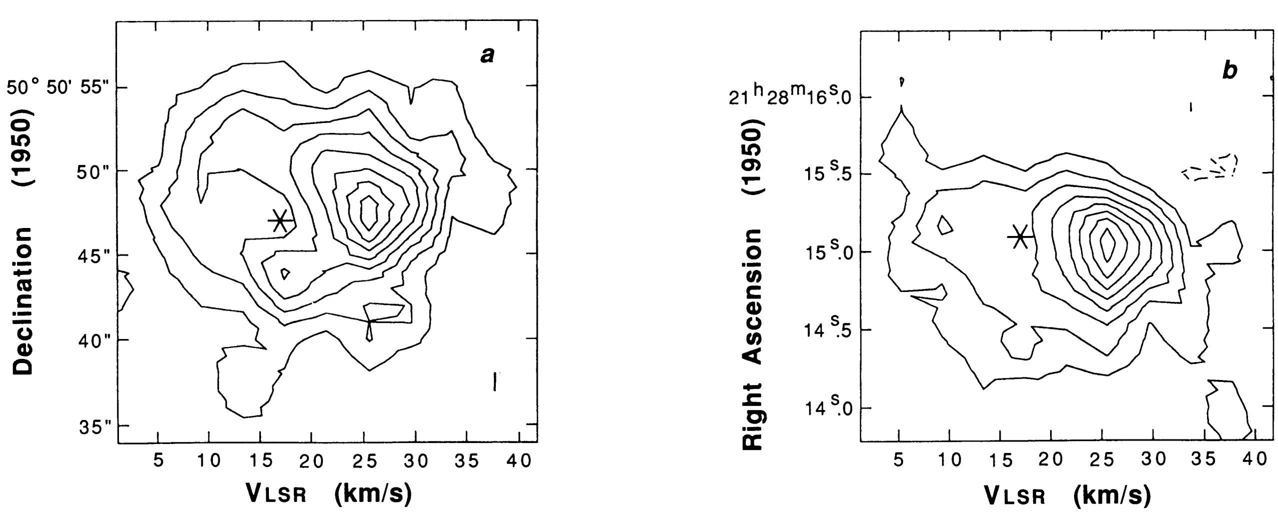

FIG. 2.—Position-velocity diagrams at position angles of 0° (*a*) and 90° (*b*) through the field center. Contour levels are in linear steps of 0.6 Jy $beam^{-1}$ (2 σ level of the maps). The position of the central star of IRAS 21282 is shown with an asterisk.

present or not, we made a map with a bandwidth of 62.5 MHz centered at 115.20 GHz which is free from contamination of CO $J = 1$–0 emission. No emission stronger than 5.1×10^{-2} Jy beam^{-1} (1 σ level of the map) was detected at the position of IRAS 21282.

III. DISCUSSION

a) Structure of CO *Gas*

For understanding the features described in § II, neither a spherically symmetric shell model nor a bipolar flow model are suitable. The simplest model which can explain the distribution and the velocity structure of CO emission is an expanding torus of CO gas. That is because (*i*) CO emission is elongated to north and south, (*ii*) the emission peaks are seen at the north and south sides of the field center on the central velocity map (Fig. 1*e*), (*iii*) the extension of CO emission in channel-velocity maps decreases with velocities away from the central velocity and its center in the channel-velocity map reveals no systematic displacement, and (*iv*) the position-velocity map at the position angle of 0° shows an asymmetric round structure surrounding the star position.

In Figure 2*a*, emission from the approaching part is weaker than the receding one. We have made position-velocity diagrams with various different right ascensions. Examining these diagrams, we can conclude that this is not resulted from the tilted torus as, for example, in NGC 2346 (Bachiller *et al.* 1989). Hence, it is suggested that the axis of the torus lies along the east-west direction and is normal to the line of sight.

The asymmetric structure in Figure 2*a* is caused by either a CO self-absorption or the real asymmetry of CO emission, or by both of them. Because the self-absorption (due to the kinetic temperature gradient in the expanding envelope) should appear at relatively lower velocities (near the low-velocity edge of line profile; $V_{\rm LSR} \lesssim 8$ km s^{-1}), the sudden drop of CO intensity at $V_{\rm LSR} \sim 8$–16 km s^{-1} cannot be explained only by the self-absorption. However, detailed radiative transport calculations and modeling of the envelope are necessary to confirm this conclusion.

b) Evolutionary Stage

Here we compare the structures of CO gas among planetary nebulae NGC 2346, NGC 7027, and IRAS 21282. In NGC 2346, Bachiller *et al.* (1989) confirmed that an expanding CO ring surrounds the central star and the waist of the bipolar-shaped ionized region. The ionized region is developed in NGC 2346 and has a comparable or slightly larger size than CO emission. Masson *et al.* (1985) suggested that the CO gas in NGC 7027 envelopes the ionized gas entirely. And, the size of the ionized gas (14″ × 9″ from Fig. 4 of Masson 1989) is much smaller than the extension of the CO gas (over 120″; see Mufson, Lyon, and Marionni 1975). In IRAS 21282, the ionized region is small ($\lesssim$1″.2 in Cohen and Jones 1987) compared with the CO gas. Actually, we could not detect the continuum emission at 115 GHz above 5.1×10^{-2} Jy beam^{-1}. Comparing these facts and, in addition, considering the line intensity ratio of [O III] λ5007 to Hβ, which was very low in IRAS 21282 (see Fig. 1 in Cohen and Jones 1987), it is suggested that IRAS 21282 is in an earlier stage of evolution than NGC 7027 is and that NGC 2346 is in the latest stage among these three objects.

Taking the distance to IRAS 21282 as D (kpc), we can estimate the kinematical age of the CO gas around IRAS 21282 as about 2070D yr using the angular radius (7″) and the expansion velocity of the CO (16 km s^{-1} from Figs. 1 and 2, and Likkel *et al.* 1988). On the other hand, we can estimate the age using the theoretical evolutionary tracks of central stars. From the line intensity ratio of [O III] λ5007 and the Kaler's (1978) empirical law, the effective temperature of the central star of IRAS 21282 is estimated to be $10^{4.5}$ K. According to Cohen and Jones (1987), the luminosity of the central star is $600D^2$ $L_\odot$. Then, if we assume the distance to IRAS 21282 to be 2 kpc (Likkel *et al.* 1988), IRAS 21282 falls near Schönberner's (1983) evolutionary track of the 0.56 $M_\odot$ central star on the H-R diagram. The age calculated from the zero-age point ($\log T_{\rm eff} = 3.7$) is 5×10^3 yr. This is in good agreement with the kinematical age of 4.1×10^3 yr, if the time duration between the starting position of mass ejection and the zero age point of Schönberner's track is neglected. When we put 4 kpc to the distance D instead of 2 kpc, the kinematical age becomes longer, 8.3×10^3 yr, and the age derived from the evolutionary track of more massive star becomes shorter, 1.5×10^3 yr. Then the coincidence becomes worse. On the other hand, when we put smaller values than 2 kpc to the distance D, the reverse trend of discrepancy occurs. Therefore, the value of the distance, 2 kpc, gives a reasonable agreement between the kinematical age of the CO gas and the age derived from the evolutionary stage of the central star with the mass of 0.56 $M_\odot$.

c) Interaction with Ionized Gas

It is important to compare the velocity structure of the molecular gas with that of ionized gas. The half-width at the zero level intensity (HWZI) of CO emission is 16 km s^{-1} in IRAS 21282 and 18 km s^{-1} in NGC 7027 (Likkel *et al.* 1988; Masson *et al.* 1985), approximately the same. But it is 37 km s^{-1} in NGC 2346 (Bachiller *et al.* 1989), considerably larger if compared with the velocities of above two objects. In NGC 2346, an optical [N II] line emission is closely associated in both position and velocity with CO emission (Healy and Huggins 1988). This association suggests that the [N II] lines are formed in the interface between the CO gas and the ionized gas, and that the CO gas constitutes the walls of the cavity in which the ionized gas is flowing (Walsh 1983; Bachiller *et al.* 1989). On the other hand, in IRAS 21282 and NGC 7027, clear features which represent the interaction between ionized gas and CO gas have not yet been obtained. Comparing with the position and the velocity of ionized gas, Masson *et al.* (1985) suggested that the high-velocity wings of CO emission in NGC 7027 arise from the gas which interacts with ionized gas.

We have now obtained the detailed structure of the CO gas around IRAS 21282. Some features may arise from the interaction with ionized gas; emisson contours at the terminal velocities of CO $J = 1$–0 emission in Figures 1*a* and 1*h* trailing from the field center symmetrically to the west and the east, respectively, along the axis of the torus. Those are weak and may be due to noise. The ionized gas in IRAS 21282 seems no bigger than 1″.2 and the expansion velocity is $\sim$12 km s^{-1} (derived from the width of optical lines; Cohen and Jones 1987). In order to conclude whether these features reveal the interaction or not, we require more information on detailed spatial and velocity structures of the interface and the ionized gas.

We would like to thank the staff of NRO for the operation of the interferometer in our observation and the support in the data reduction.

REFERENCES

Bachiller, R., Planesas, P., Martín-Pintado, J., Bujarrabal, V., and Tafalla, M. 1989, *Astr. Ap.*, **210**, 366.
Bieging, J. H., and Nguyen-Q-Rieu. 1988, *Ap. J.*, **324**, 516.
Chikada, Y., *et al.* 1987, *Proc. IEEE*, Vol. **75**, No. 9, 1203.
Cohen, M., and Jones, B. F. 1987, *Ap. J.* (*Letters*), **321**, L151.
de Muizon, M., Geballe, T. R., d'Hendecourt, L. B., and Bass, F. 1986, *Ap. J.* (*Letters*), **306**, L105.
Healy, A. P., and Huggins, P. J. 1988, *A.J.*, **95**, 866.
Heiligman, G. M., *et al.* 1986, *Ap. J.*, **308**, 306.
Huggins, P. J., and Healy, A. P. 1986, *M.N.R.A.S.*, **220**, 33P.
Ishiguro, M., *et al.* 1984, in *Proc. Int. Symposium Millimeter and Submillimeter Wave Radio Astronomy* (Granada), p. 75.
Kaler, J. B. 1978, *Ap. J.*, **220**, 887.
Kawabe, R., *et al.* 1987, *Ap. J.*, **314**, 322.
Knapp, G. R. 1985, in *Mass Loss from Red Giants*, ed. M. Morris and B. Zuckerman (Dordrecht: Reidel), p. 171.
Likkel, L., Forveille, T., Omont, A., and Morris, M. 1988, *Astr. Ap.*, **198**, L1.
Masson, C. R. 1989, *Ap. J.*, **336**, 294.
Masson, C. R., *et al.* 1985, *Ap. J.*, **292**, 464.
Mufson, S. L., Lyon, J., and Marionni, P. A. 1975, *Ap. J.* (*Letters*), **201**, L85.
Nagata, T., Tokunaga, A. T., Sellgren, K., Smith, R. G., Onaka, T., Nakada, Y., and Sakata, A. 1988, *Ap. J.*, **326**, 157.
Schönberner, D. 1983, *Ap. J.*, **272**, 708.
Thronson, H. A., and Mozurkewich, D. 1983, *Ap. J.*, **271**, 611.
Walsh, J. R. 1983, *M.N.R.A.S.*, **202**, 303.

S. Deguchi, N. Hirano, O. Kameya, T. Kasuga, and K. M. Shibata: Nobeyama Radio Observatory, National Astronomical Observatory, Nobeyama, Minamimaki, Minamisaku, Nagano 384-13, Japan

S. Tamura: Astronomical Institute, Tohoku University, Aoba, Aramaki, Aoba, Sendai 980, Japan